Giant bistable shifts for one-dimensional nonlinear photonic crystals

Peng Hou,* Yuanyuan Chen, Xi Chen, Jielong Shi, and Qi Wang
Department of Physics, Shanghai University, Shanghai 200444, People's Republic of China
(Received 8 January 2007; published 26 April 2007)

It is found that there exists a hysteretic response between the incident intensity and the lateral shift for a one-dimensional photonic crystal containing a nonlinear defect. The lateral shift can be greatly enhanced when the incident intensity decreases from a value higher than the switch-up threshold of optical bistability and reaches the maximum at the switch-down threshold. It is also found that the hysteresis is strongly dependent on the nonlinear defect, the incident angle, and the incident frequency. The validity of the theoretical analysis is demonstrated by numerical simulations for a Gaussian beam.

DOI: 10.1103/PhysRevA.75.045802 PACS number(s): 42.25.Gy, 42.25.Bs, 78.20.Bh, 42.70.Qs

In the past few years, photonic crystals (PCs) [1] have inspired considerable interest in both physics and engineering communities because such periodic structures can enable many interesting electromagnetic behaviors, such as the superprism phenomenon [2–5] and the ultrarefractive effect [6–9]. The Goos-Hänchen (GH) shift is known as a lateral shift from the path usually expected from geometrical optics when a light beam is totally reflected from the interface of two different media [10]. Recently, GH shifts in PCs have attracted much attention [11–13]. Felbacq *et al.* have shown that obvious GH shifts exist for PCs at frequencies both inside and outside a band gap [11]. Giant negative GH shifts for a PC with a negative refractive index are also discussed [12]. These results have potential applications in integrated optics.

It has been reported that when a light beam is incident on a 1D PC containing a linear defect layer, lateral shifts can be greatly enhanced near the defect mode [13]. However, the frequency band for greatly improved lateral shifts is too narrow. It is well known that if the defect has nonlinearity, strong nonlinear effect that happened in the defect may change the defect mode frequency [14]. It is expected that lateral shifts in a much wider frequency region can be remarkably enhanced. In this paper, we investigate the influence of the nonlinear defect on GH shifts for a 1D PC.

We use the symmetric multilayer stack [13] consisting of two alternate linear layers A and B as our 1D PC structure. (See Fig. 1) Now we replace the middle linear defect layer by a Kerr-type nonlinear layer, for which the effective index of refraction can be written in the form of $n^2=n_D^2+\chi_3|E(z)|^2$. Here n_D is the linear refractive index of the nonlinear material, χ_3 is the nonlinear coefficient. The alternating layers have a high refractive index n_A and a low refractive index n_B. Assume that all the layers are dielectric materials and their thicknesses satisfy $n_Ad_A=n_Bd_B=\lambda_{PC}/4$. Such structure can create a band gap with center frequency $2\pi c/\lambda_{PC}$ at normal incidence.

Suppose a wave beam of angular frequency ω incident from vacuum upon a finite 1D PC at an angle θ. Here we only consider the TE-polarized waves. The treatment for TM waves is similar. From Maxwell's equations, the x component of the electric field and the y component of the magnetic field at two sides of the jth Kerr-type nonlinear layer of width d_j can be related by the following equation [15]

$$\begin{bmatrix} E_x(z) \\ -H_y(z) \end{bmatrix} = M_j(k_y)\begin{bmatrix} E_x(z+d_j) \\ -H_y(z+d_j) \end{bmatrix}, \tag{1}$$

and

$$M_j(k_y)=\frac{k}{k_{j+}+k_{j-}}\begin{bmatrix} \frac{k_{j-}}{k}\exp(-ik_{j+}d_j)+\frac{k_{j+}}{k}\exp(ik_{j-}d_j) & \exp(-ik_{j+}d_j)-\exp(ik_{j-}d_j) \\ \frac{k_{j-}k_{j+}}{k^2}[\exp(-ik_{j+}d_j)-\exp(ik_{j-}d_j)] & \frac{k_{j+}}{k}\exp(-ik_{j+}d_j)+\frac{k_{j-}}{k}\exp(ik_{j-}d_j) \end{bmatrix}, \tag{2}$$

where k_{j+} and k_{j-} are the propagation constants of the forward and backward propagating waves and are given by

$$k_{j_\pm}=\sqrt{(kn_j)^2-(k_y)^2}(1+U_{j\pm}+2U_{j\mp})^{1/2}, \tag{3}$$

with $k=\omega/c$, k_y is the y component of the incident wave vector and

*Email address: houpengshu@126.com

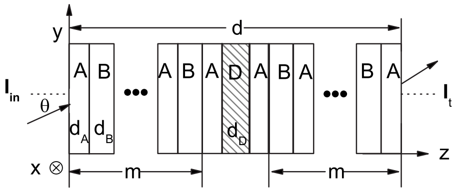

FIG. 1. Schematic of a 1D PC with a nonlinear defect. m represents the number of periods. d is the thickness of the multilayer.

$$U_{j\pm} = \frac{k^2\chi_3}{n_j^2 k^2 - k_y^2}|A_{j\pm}|^2. \quad (4)$$

Here A_{j+} and A_{j-} are amplitudes of the forward and backward waves and n_j is the linear refractive index. When $\chi_3 \neq 0$, the wave vectors k_{j+} and k_{j-} depend on U_{j+} and U_{j-}. Therefore, to have the explicit form of $M_j(k_y)$, one has to solve a set of coupled nonlinear equations with respect to U_{j+} and U_{j-} for a given transmitted intensity by using fixed point iteration [16]. In our computations, we take $U_{j\pm}=0$ as the initial values and 1000 iterations to find the stable solutions. Once $U_{j\pm}$ are determined, the characteristic matrix for the nonlinear layer can be calculated using formulas (2) and (3). Then the characteristic matrix for the composite medium can be written as

$$M(k_y) = \prod_{j=1}^{2m+3} M_j(k_y), \quad (5)$$

where $M_j(k_y)$ is given by Eq. (2). It is noted that Eq. (2) in the linear case ($\chi_3=0$) reduces to the standard form of characteristic matrix [17]. Then the transmission coefficient can be given by

$$t(k_y) = \frac{2p_f(k_y)}{[M_{11} + M_{12}p_f(k_y)]p_f(k_y) + [M_{21} + M_{22}p_f(k_y)]}, \quad (6)$$

where $p_f(k_y)=(k^2-k_y^2)^{1/2}/k$ and $M_{ij}(k_y)$ are the elements of 2×2 matrix $M(k_y)$. From Eq. (6), the phase shift of the transmitted beam with respect to the incident beam can be obtained

$$\phi(k_y) = \tan^{-1}[\mathrm{Im}\, t(k_y)/\mathrm{Re}\, t(k_y)], \quad (7)$$

For an incident beam that is sufficiently wide, the lateral shift Δ of the transmitted beam through the multiple layered structure can be calculated analytically as [13,18]

$$\Delta = -\, d\phi(k_y)/\, dk_y|_{\theta=\theta_0}. \quad (8)$$

For a given transmitted intensity, one can calculate the incident intensity through the power transmittance $T=tt^*$.

The numerical calculation result for the relation of the incident and transmitted intensities is shown in Fig. 2(a), in which a typical S-shaped curve indicates that such composite structure can produce an optical bistability (OB). The parameters are taken as follows: $n_A=2.3$, $n_B=1.308$, $\lambda_{PC}=3$ mm, $\chi_3=0.01$, $n_D=1.594$, $d_D=0.94$ mm, $\theta=30°$, $\omega/2\pi=103.5$ GHz, and $m=3$. I_{up} and I_{down} represent the switch-up and switch-down threshold values for OB, respectively. We plot the variation of the corresponding lateral shift for wide beam with the incident intensity I_{in} in Fig. 2(b), from which a hysteretic response of Δ and I_{in} can be found. Relating with Fig. 2(a), it is noted that Δ is greatly enhanced when I_{in} decreases from a value higher than I_{up} (about 1.662) and reaches the maximum at I_{down} (about 0.221). It is interesting to find that the variation of Δ with respect to I_{in} is very similar to the transmittance T as a function of I_{in}.

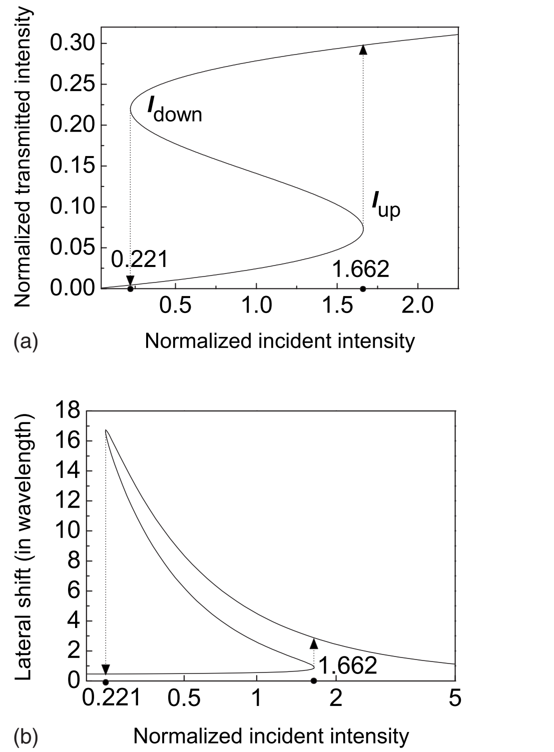

FIG. 2. The variations of (a) the normalized transmitted intensity and (b) the lateral shift, with the normalized incident intensity. The linear refractive index and the thickness of the nonlinear defect are chosen to be $n_D=1.594$ and $d_D=0.94$ mm; the incident angle is 30°; the incident wave frequency is $\omega/2\pi=103.5$ GHz.

To understand this more clearly, we have investigated ϕ with respect to k_y for different I_{in} as is shown in Fig. 3. We can observe that around some fixed k_y (e.g., $k_y/k=0.5$) ϕ experiences a distinct sharp variation as I_{in} first increases and then decreases. Thus, the hysteretic behavior of Δ with the variation of I_{in} can be explained easily. In the beginning, I_{in} increases slowly from zero, the variation of ϕ becomes sharp slowly, and when I_{in} reaches I_{up}, ϕ will jump to a higher value. After that, further increasing of I_{in} will cause the variation of ϕ to become gentle slowly. In contrast, when I_{in} decreases slowly from a high value, the variation of ϕ becomes sharp gradually. When I_{in} decreases to I_{up}, ϕ will not jump back to the lower value immediately, but continues to decrease slowly until I_{in} reaches another threshold intensity I_{down}. At this time, ϕ will suffer a most abrupt change, which leads to the largest value of Δ. Then ϕ suddenly jumps back to a continuous state with a small slope and the slope becomes smaller and smaller with decreasing of I_{in}.

In the following, we discuss the dependence of the hysteresis on the nonlinear material and the incident beam. The calculated dependence of lateral shifts on I_{in} with various n_D

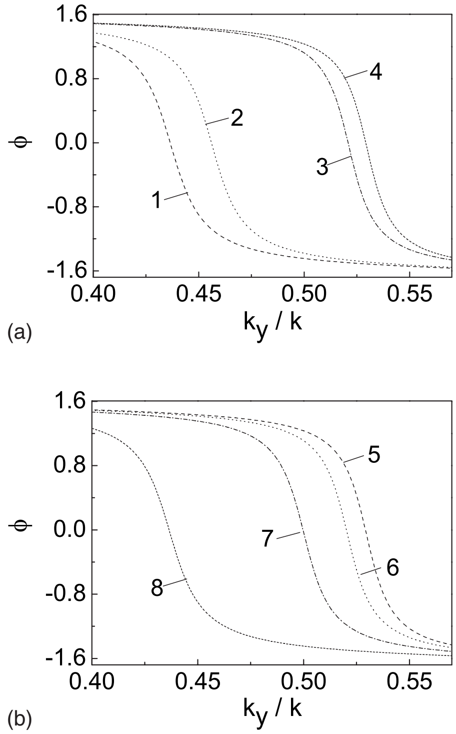

FIG. 3. Phase shift as a function of k_y with various I_{in}. k_y is rescaled by k_y/k. (a) When I_{in} increases from zero; (b) when I_{in} decreases from a value higher than I_{up}. The numbers in the panels represent different values of the incident intensities: I_{in}=(1) 0.2199; (2) 1.6622; (3) 1.6628; (4) 3.4557; (5) 3.4557; (6) 1.6543; (7) 0.2212; (8) 0.2199. The other parameters are the same as Fig. 2.

of the nonlinear defect is shown in Fig. 4. From this figure, we can observe that when n_D=1.594, Δ is mostly improved near I_{down} and with increasing of n_D in integer times, the peak of the hysteresis decreases. On the other hand, a similar situation occurs if we change the thickness of the nonlinear material. However, at this case the hysteresis becomes sharper and sharper as the thickness of the nonlinear defect increases in integer times.

It is well known that the defect mode frequency Ω depends on the structure and incident angle. In the case of the linear structure, for fixed ω lateral shifts can be greatly enhanced at some incident angle and decreases drastically as the angle deviates away from the center value [13]. How about the nonlinear case? Figure 5 displays lateral shifts at several incident angles. It is very clear that the peak of the hysteresis becomes larger and larger with the increment of the incident angle, which is very different from the linear structure.

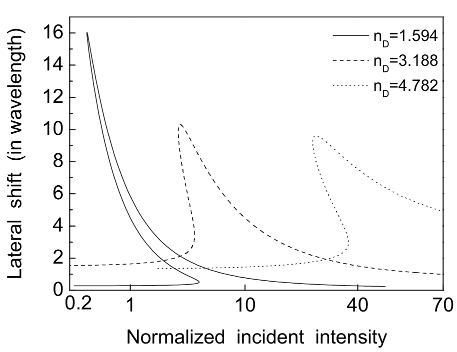

FIG. 4. The dependence of Δ on I_{in} for various n_D of the nonlinear defect. Solid curve, n_D=1.594; dashed curve, n_D=3.188; dotted curve, n_D=4.782. The incident wave frequency is taken as $\omega/2\pi$=103 GHz. Other parameters as in Fig. 2.

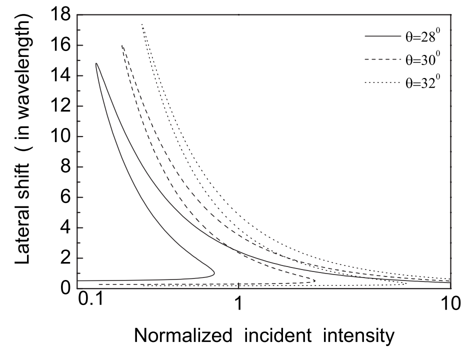

FIG. 5. The dependence of Δ on I_{in} at several incident angles. Solid line, θ=28°; dashed line, θ=30°; dotted line, θ=32°. The incident wave frequency is taken as $\omega/2\pi$=103 GHz and other parameters are the same with Fig. 2.

In Ref. [13], the great enhancement of Δ occurs only near the defect mode. Our calculation results show that lateral shifts of a much wider frequency band can be greatly enhanced near I_{down}. It is very interesting to find that the hysteretic behavior is dependent of the frequency offset between ω and Ω_0 (which is determined only by n_D). Figure 6 displays the peaks of the hystereses for some frequencies, from which we can observe that the peak of the hysteresis increases rapidly as ω comes close to Ω_0 (here $\Omega_0/2\pi$ is about 105 GHz). This is because that strong Kerr effect inside the defect structure causes the defect mode to shift to ω [14]. The closer ω comes to Ω_0, the more abrupt the change is, which is experienced by ϕ near I_{down}. However, if ω comes very close to or even exceeds Ω_0, since I_{up} and I_{down} cannot form a bistability cycle, the hysteretic response between Δ and I_{in} will disappear.

To demonstrate the validity of the above analysis, numerical simulations have been performed. We assume that a 1D PC is illuminated by a Gaussian-shaped beam, which can be expressed by the Fourier integral as follows

$$\Psi_{\mathrm{in}}(\vec{z})|_{z=0} = \frac{1}{\sqrt{2\pi}} \int A(k_y)\exp(ik_y y)dk_y, \tag{9}$$

where $A(k_y)=w_y \exp[-w_y^2(k_y-k_{y0})/4]/\sqrt{2}$ is the Fourier spectrum of the incident beam, $w_y=w_0 \sec\theta$, w_0 is the beam width at the waist, and $k_{y0}=k\sin\theta$. Then the field of the transmitted beam is given by

$$\Psi_t(\vec{z}) = \frac{1}{\sqrt{2\pi}} \int tA \exp[ik_z(z-d) + ik_y y]dk_y. \tag{10}$$

The integration above is performed from $-k$ to k. The lateral shift can be obtained by finding the location where the field is the maximum [18].

The calculation results show that our theoretical analysis

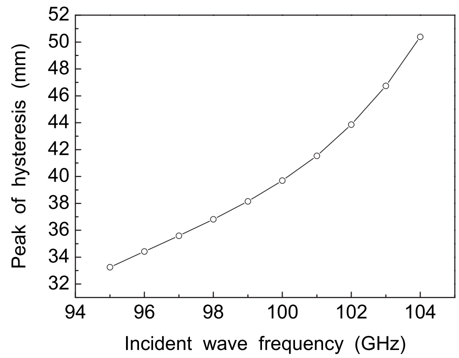

FIG. 6. Peaks of the hystereses for different incident frequencies. Other parameters as in Fig. 2.

are in good agreement with the numerical results. The discrepancy between the numerical and theoretical results is due to the distortion of the transmitted Gaussian beam. Such distortion gradually disappears as w_0 becomes larger as is shown in Fig. 7(b). In order to guarantee the validity of the approximate formula (8), it is required that ϕ is a linear function of k_y across the interval of k_y, where the angular distribution is applicable. Further numerical computations show that the wider the Gaussian beam waist is, the more linearly ϕ depends on k_y, and the better the transmitted beam retains the shape of the incident beam.

In summary, we have investigated lateral shifts of the transmitted beams for a 1D PC doped with a nonlinear defect layer. Lateral shifts of a wide frequency band are greatly improved near I_{down} of OB. Choosing a nonlinear material with a lower linear refractive index or a bigger thickness or bigger incident angle is helpful to obtain larger lateral shifts. For fixed structure and incident angle, the dependence of lateral shifts on I_{in} is determined by the frequency offset between ω and Ω_0, which can be applied to a wavelength demultiplexer. Numerical simulations for a Gaussian beam have been performed to confirm the validity of theoretical results. For a Kerr-type nonlinearity with negative sign, the results are similar, but we need to tune ω at the other side of Ω_0. These conclusions add different features to the domain of nonlinear Goos-Hänchen shifts [19].

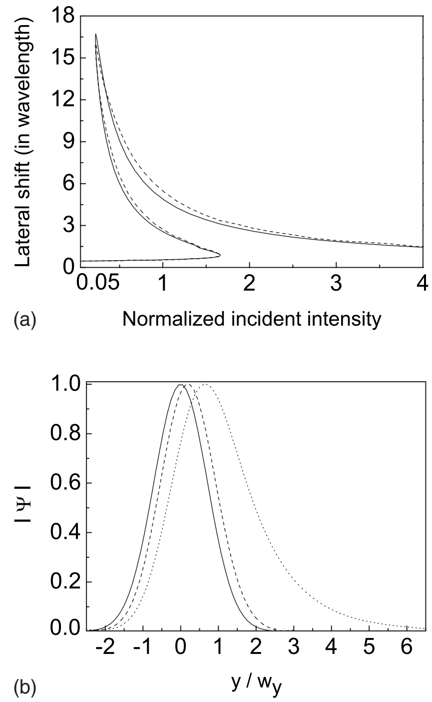

FIG. 7. (a) The comparison between the theoretical and numerical results of lateral shift with respect to I_{in}. Solid curve, theoretical result; dashed curve, numerical result. (b) The normalized profiles of the Gaussian-shaped incident and transmitted beams at $z=d$. Solid curve, incident beam; dashed curve, transmitted beam for $w_0=70\lambda$; dotted curve, transmitted beam for $w_0=12\lambda$. The incident intensity is 0.221. Other parameters as in Fig. 2

This work was supported in part by the National Natural Science Foundation of China (Grants No. 60677030 and 60377025), Science and Technology Commission of Shanghai Municipal (Grants No. 06ZR14034 and 04JC14036), and the Shanghai Leading Academic Discipline Program (T0104).

[1] J. D. Joannopoulos, R. D. Meade, and J. N. Winn, *Photonic Crystals: Modeling the Flow of Light* (Princeton University Press, Princeton, NJ, 1995).

[2] S. Y. Lin, V. M. Hietala, L. Wang, and E. D. Jones, Opt. Lett. **21**, 1771 (1996).

[3] H. Kosaka, T. Kawashima, A. Tomita, M. Notomi, T. Tamamura, T. Sato, and S. Kawakami, Phys. Rev. B **58**, R10096 (1998).

[4] P. Halevi, A. A. Krokhin, and J. Arriaga, Appl. Phys. Lett. **75**, 2725 (1999).

[5] T. Baba and M. Nakamura, IEEE J. Quantum Electron. **38**, 909 (2002).

[6] C. G. Parazzoli, R. B. Greegor, K. Li, B. E. C. Koltenbah, and M. Tanielian, Phys. Rev. Lett. **90**, 107401 (2003).

[7] E. Cubukcu, K. Aydin, E. Ozbay, S. Foteinopolou, and C. M. Soukoulis, Nature (London) **423**, 604 (2003).

[8] I. Bulu, H. Caglayan, and E. Ozbay, Phys. Rev. B **72**, 045124 (2005).

[9] R. Gajić, R. Meisels, F. Kuchar, and K. Hingerl, Phys. Rev. B **73**, 165310 (2006).

[10] F. Goos and H. Hänchen, Ann. Phys. **1**, 333 (1947); **5**, 251 (1949).

[11] D. Felbacq, A. Moreau, and R. Smaali, Opt. Lett. **28**, 1633 (2003); D. Felbacq and R. Smaâli, Phys. Rev. Lett. **92**, 193902 (2004).

[12] J. He, J. Yi, and S. He, Opt. Express **14**, 3024 (2006).

[13] L.-G. Wang and S.-Y. Zhu, Opt. Lett. **31**, 101 (2006).

[14] H. Inouyea and Y. Kanemitsu, Appl. Phys. Lett. **82**, 1155 (2003).

[15] S. Dutta Gupta, J. Opt. Soc. Am. B **6**, 1927 (1989).

[16] S. Dutta Gupta and D. S. Ray, Phys. Rev. B **38**, 3628 (1988).

[17] M. Born and E. Wolf, *Principles of Optics* (Pergamon, New York, 1970).

[18] X. Chen and C.-F. Li, Phys. Rev. E **69**, 066617 (2004).

[19] M. Peccianti, A. Dyadyusha, M. Kaczmarek, and G. Assanto, Nat. Phys. **2**, 737 (2006).